Nanorheology of strongly confined oligomeric lubricants

Manias, E.; Brinke, G. ten; Hadziioannou, G.

Published in:
Journal of Computer-Aided Materials Design

DOI:
10.1007/bf01185670

Publication date:
1996

Journal of Computer-Aided Materials Design, 3 (1996) 319–328
ESCOM

J-CAMATD 056

Nanorheology of strongly confined oligomeric lubricants

E. Manias*, G. ten Brinke and G. Hadziioannou

Laboratory of Polymer Chemistry and Materials Science Center, University of Groningen, Nijenborgh 4, 9747 AG Groningen, The Netherlands

Received 8 January 1996
Accepted 15 January 1996

Keywords: Polymer rheology; Fluid lubricants; Nanometer confinements; Molecular dynamics simulations

SUMMARY

Lubricant films confined in nanometric slit pores and subjected to shear flow are studied by non-equilibrium molecular dynamics in a planar Couette flow geometry. An inhomogeneous, layered density profile is developed near the confining surfaces and the shape of the velocity profile across the pore depends on the wall energetics. A nonlinear velocity profile is developed and both slippage located at the wall and inside the film (interlayer slip) are observed. The local slope of the velocity profile and the location of the slippage plane are determined by the adsorption energy of the wall. Shear-induced changes of the adsorbed chain conformations are discussed in relation with the molecular mechanism of slippage and the magnitude of the interlayer slip.

INTRODUCTION AND METHOD

Lubrication, friction and adhesion are of great importance to many technological applications. Due to the increasing miniaturization of high-technological devices, the dimensional tolerances approach the nanometer scale and necessitate an understanding at the microscopic (molecular/atomic) scale; thus, the molecular aspects of friction and lubrication become central in major technological and economical problems [1,2]. Still there remain many unanswered questions in the fields of nanotribology and nanorheology [3,4], especially on how the behaviour at the molecular scale determines the macroscopic response of lubricating or adhesive films. Advances in experimental techniques, like the *friction* Atomic Force Microscope [5] and the *shearing* Surface Forces Apparatus (SFA) [6–8], have provided the ability to experimentally obtain information on friction at the atomic scale and, complemented by atomistic simulations, have made considerable progress towards the understanding of how lubricants behave at the molecular level [1].

*To whom correspondence should be addressed at: Materials Science and Engineering Department, Cornell University, Bard Hall, Ithaca, NY 14853-1501, U.S.A.

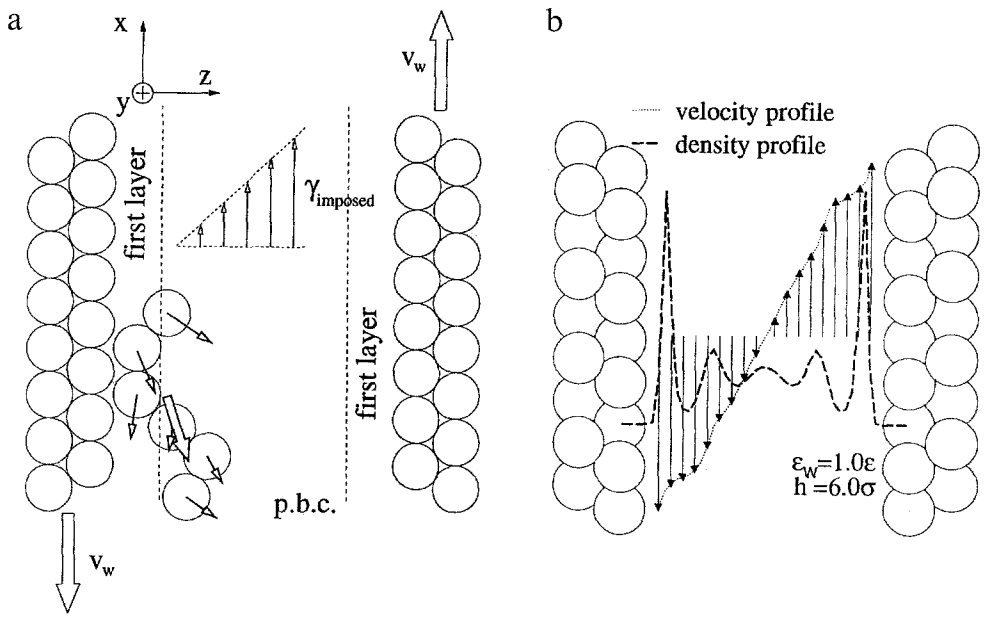

Fig. 1. Schematic representation of the simulated system: (a) Simulation geometry: the velocity gradient and flow are parallel to **z** and **x**, respectively. (b) Velocity profile definition: after dividing the film in z slices, the **x** projection of the particle velocity is averaged in each slice.

These advances made study of the properties of ultrathin films possible, by providing direct measurements and new insights into molecular- and atomic-level processes of the structural and dynamic properties of surfaces and interfaces, which are essential for an educated guess for the design and engineering of new higher performance materials. In the present study, an effort is made towards the understanding of the rheology of these nanoscopically confined fluid films, with an emphasis on the connection between the conformational changes of the adsorbed oligomers (molecular scale) and the rheological behaviour of the lubricating film (continuum scale).

The systems studied are confined films of oligomers with mainly 6 (hexamers) or 10 (decamers) segments per chain. The details of the simulations have been presented elsewhere [14–17] and will only be briefly mentioned here.

The chains are modelled by an abstract and generic, though well-studied, bead-spring model [9–13] confined between two double-layered (111) fcc surfaces normal to $\vec{z}$ and periodic boundary conditions imposed in the other two directions (Fig. 1a). Shear is imposed by moving the walls with a constant velocity (v_w) towards opposite directions ($\pm\vec{x}$, Fig. 1) while they are kept at constant separation (NVT ensemble). The interactions between the particles are modelled by the Lennard-Jones (LJ) potential, truncated at a distance $r_c = \sqrt[6]{2}\,\sigma$:

$$U(r) = \begin{cases} 4\varepsilon\left((\sigma/r)^{12} - (\sigma/r)^{6} + 1/4\right) & \text{for } r \le \sqrt[6]{2}\,\sigma \\ 0 & \text{for } r \ge \sqrt[6]{2}\,\sigma \end{cases} \qquad (1)$$

where ε is the LJ energy parameter and σ the LJ length parameter. Connectivity along the chains is realized by adding a strongly attractive FENE (Finite Extensibility Non-Elastic) potential

between successive beads along one chain:

$$U_{conn}(r) = -(k/2)R_0^2 \ln(1-(r/R_0)^2) \quad \text{for } r < R_0 \tag{2}$$

where $R_0 = 1.5\sigma$ and $k = 30.0\varepsilon/\sigma^2$. These potentials have been used before in extensive studies of bulk systems [13], under confinement between walls [9,11], as well as under shear [10–16], and reproduce many static and dynamic properties of polymer systems. This choice of parameters for the FENE potential has been proven to produce realistic chain dynamics, preventing bond crossing and bond breaking, even at temperatures higher than the one used in our simulation [13]. The temperature is kept constant at $k_B T = 1.0\,\varepsilon$ with the use of the Berendsen thermostat [18]. The interactions between the walls and the segments are modelled by the *full* Lennard-Jones potential, which includes an attractive tail:

$$U_w(r) = 4\varepsilon_w((\sigma_w/r)^{12} - (\sigma_w/r)^6) \tag{3}$$

By changing the value of ε_w, the strength of the wall attraction can be varied systematically: from neutral walls ($\varepsilon_w = 0.0$), weakly adsorbing surfaces ($\varepsilon_w = 1.0\varepsilon$) to strongly adsorbing surfaces ($\varepsilon_w \geq 2.0\varepsilon$) [11,15]. In order to reduce the computational effort, this potential is truncated at $r_{wc} = 2.5\sigma$.

RESULTS AND DISCUSSION

From the first SFA studies, it was established that confined fluids are strongly inhomogeneous in the vicinity of the confining surfaces, both for systems of small molecules [21,22] and of long polymers [23,24], giving rise to wildly oscillating solvation forces. This inhomogeneity (strong density variations normal to the walls) is captured by MD computer simulations (Fig. 2; see also Ref. 9) and is of the same physical origin as the oscillations in the radial distribution function

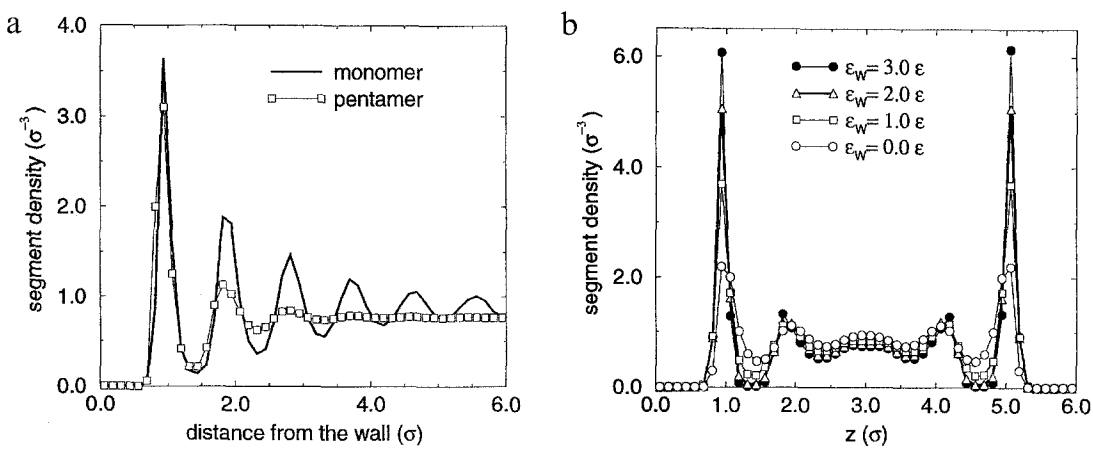

Fig. 2. (a) Number density of segments normal to one confining surface located at the origin. The systems correspond to an LJ fluid and a pentamer bead-spring melt of the same average density ($\varepsilon_w = 1.0\varepsilon$). (b) When the system is confined between *two* walls, inhomogeneity is observed next to both surfaces. Density profiles are given of confined hexamers for various wall attractions ($h = 6.0\sigma$, confining surfaces located at $z = 0.0$ and $z = 6.0$).

of simple liquids. It can be explained fairly easily for the reference system of a hard-sphere fluid next to a hard wall; when a hard sphere is adjacent to the wall, then the collisions with other fluid particles from the side facing the surface are much more frequent than from the side of the wall. In this way, the rest of the fluid particles, acting as a heat bath, give rise to a net force pushing this particle towards the wall. Thus, the particles touching the surface are effectively attracted to it due to the angular asymmetry of their collisions with the other fluid particles. Exactly this idea is exploited to interpret the oscillations of the radial pair correlation function [19], and the 'potential of mean force' is defined as the interaction between two particles when the rest of the system is canonically averaged over all configurations. This potential exhibits attractive minima, even in the case of hard spheres. Similarly, for attractive surfaces there is an effective mean force potential and, moreover, the interatomic potential between the wall atoms and the fluid particles is added to it, resulting in an increase of the density oscillations near the wall. The comparison of the density profiles of an oligomer melt with a monomeric fluid shows two main features (Fig. 2a): (i) the density of the first layer is larger for the monomeric fluid than for the oligomer; (ii) the density oscillations for the oligomer melt are damped much faster than those of the simple liquid. In fact, even for the relatively short chain (pentamer) shown in Fig. 2, only two fluid layers are developed next to the surface, whereas for the monomer layering is quite strong, even beyond six fluid layers.

Both of these differences are directly mirrored to the oscillations of the solvation forces, which are smaller in the case of chain molecules and also damped much faster than the oscillations in the solvation forces of the simple liquids [23]. Obviously, these differences originate from the *connectivity* between consecutive segments along the chains, since the rest of the interactions are the same in the two systems, and are not enhanced with further increase of the chain size, up to the entanglement length [9].

Even more important than the wildly fluctuating density profiles are the average densities per layer (Table 1). It is clear that, when the wall affinity becomes stronger, apart from the inhomogeneity enhancement constituted by larger variations of the *local* segment density (Fig. 2), there is also an increase of the *average* segment density inside the first layer (Table 1). These average segment densities per layer have been proven to affect the segment mobility in a much more direct way than the local densities [11,20,25,26] and seem to be the origin of the 'glassy' dynamics in the solid–oligomer interface [11,15]. Moreover, this wall-induced densification inevitably causes an enhancement of the in-plane ordering in order for more segments to be accommodated inside the first layer.

Since theories predicting velocity profiles of strongly inhomogeneous systems are in an early stage of development [25,26], one of the first questions to be addressed concerns the shape of the

TABLE 1
AVERAGE SEGMENT DENSITIES PER LAYER

Layer	$h = 7.0\sigma$, $\varepsilon_w = 1.0$	$h = 6.0\sigma$			
		$\varepsilon_w = 0.0$	$\varepsilon_w = 1.0$	$\varepsilon_w = 2.0$	$\varepsilon_w = 3.0$
First	1.01	0.95	1.05	1.18	1.26
Second	0.74	0.80	0.73	0.74	0.79
Third	0.78	0.82	0.80	0.75	0.70

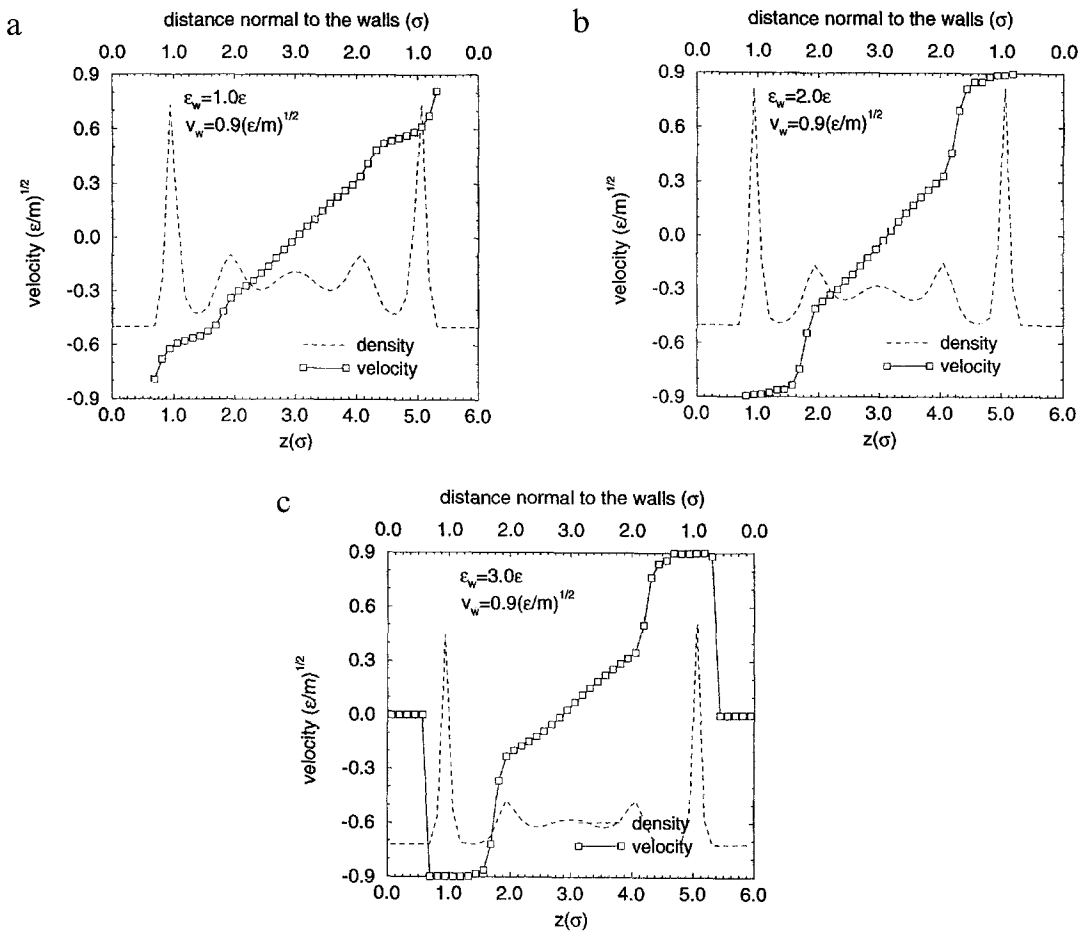

Fig. 3. The velocity profile changes qualitatively with the wall affinity between systems with (a) weakly ($\varepsilon_w = 1$) and (b and c) strongly (b: $\varepsilon_w = 2$, c: $\varepsilon_w = 3$) physisorbing surfaces. Further increase of the wall attraction beyond $\varepsilon_w = 2$ does not change the shape of the velocity profile qualitatively and results only in quantitative differences. The systems presented are in equally wide pores ($h = 6\sigma$), with the same average density and pressure, and the same shear rate $\dot{\gamma} = 0.3(\varepsilon/\sigma^2 m)^{1/2}$ is imposed.

velocity profile in confined systems under a steady shear rate. The flow field of a confined oligomer melt can be described by the mean flow velocities of the confined oligomers after steady-state flow has been established. The velocity profile can be defined as:

$$\mathbf{v}(z) = \left\langle \frac{1}{N(z,t)} \sum_{i=1}^{N(z,t)} \mathbf{v}_{i(z,t)} \right\rangle \tag{4}$$

where $\mathbf{v}(z)$ is the average velocity of all particles located in a thin slice at a distance z away from the wall, N(z,t) is the number of segments in the slice at time t and $\mathbf{v}_i(z,t)$ is the velocity of particle i at time t (Fig. 1b). The averaging over time is essential to distinguish the flow component inside the instantaneous velocities, which is screened by the random thermal velocities. In

weak flow fields, this requires very demanding runs over extremely long periods. As a result, non-equilibrium molecular dynamics (NEMD) simulations are restricted to the strong shear rates region, even for the most powerful computers available.

Figure 3 shows the velocity profiles developed in our Couette flow geometries across pores between surfaces of different wall affinities. The velocity profiles are superimposed on the corresponding density profiles and the figure borders are the positions of the walls ($z = 0$ and h) and the wall velocities (velocity $= \pm v_w$). The velocity profiles are not linear, as would be expected from the hydrodynamics of Couette flow in the bulk [27], but they do not follow the wild density variations either. In fact, they are more smooth than the velocity profiles obtained in similar geometries for monomers [28–31]. For monomeric systems the density profiles are more layered in the first place and, furthermore, the monomers develop a nonlinear, 'ragged' velocity profile [25,28], as each monomeric layer can flow with a different velocity, resulting in a 'stairway'-like velocity profile [28]. Local density approximation theories [25] also predict this kind of velocity profiles for monomers. In all cases, for the oligomers the velocity profile is linear inside the middle part of the system, where the density is almost constant (Fig. 3). In the vicinity of the surface, the velocity profile changes drastically with the wall energetics.

For moderately attractive walls (Fig. 3a), the velocity profile is almost linear inside the adsorbed layer, but with a smaller slope than in the middle part of the system. This implies that in the interfacial region the effective viscosity is higher than in the middle of the film [17]. Moreover, slip appears between the wall and the fluid (slip boundary conditions at the wall). Some time ago, De Gennes [32] established that a polymer or an oligomer melt flowing past a smooth, nonadsorbing surface would always slip. As these complex fluids exhibit an enhanced ability to resist flow (in comparison with simple LJ fluids), slip appears at the wall, even for surfaces that possess a moderate attraction ($\varepsilon_w = 1.0$; Fig. 3a).

The molecular mechanism responsible for the slippage at a surface is quite well understood [32,34,35] and intuitively expected. Slippage at the wall takes place when a smooth and weakly adsorbing surface is moving past a fluid that is characterized by some kind of physical cohesion. Thus, in the absence of surface roughness and of strong surface attraction, the fluid in contact with the surfaces cannot exactly follow the motion of the surface, but is slowed down due to its physical connectivity with the slower moving fluid located further away from the walls; as a

TABLE 2
PROBABILITIES OF CONFORMATIONS WITH A SPECIFIC NUMBER OF CONTACTS FOR ADSORBED HEXAMERS

No. of contacts	Wall velocity ($\varepsilon_w = 1.0$)				Wall velocity ($\varepsilon_w = 2.0$)				Wall velocity ($\varepsilon_w = 3.0$)			
	0.00	0.20	0.50	10.5	0.00	0.20	0.50	20.0	0.00	0.20	0.50	2.0
1	0.12	0.11	0.11	0.10	0.07	0.05	0.05	0.05	0.07	0.09	0.02	0.03
2	0.17	0.15	0.13	0.11	0.10	0.08	0.07	0.05	0.11	0.09	0.04	0.05
3	0.19	0.17	0.14	0.12	0.14	0.14	0.10	0.06	0.13	0.09	0.08	0.05
4	0.18	0.18	0.17	0.16	0.17	0.17	0.12	0.07	0.17	0.15	0.04	0.06
5	0.18	0.19	0.21	0.21	0.22	0.24	0.17	0.12	0.23	0.10	0.15	0.06
6	0.16	0.20	0.24	0.30	0.30	0.32	0.49	0.65	0.29	0.48	0.67	0.75

The adsorbed hexamers are confined between weakly ($\varepsilon_w = 1$) and strongly ($\varepsilon_w = 2$ and $\varepsilon_w = 3$) physisorbing walls for several imposed wall velocities. For all systems, $h = 6\sigma$.

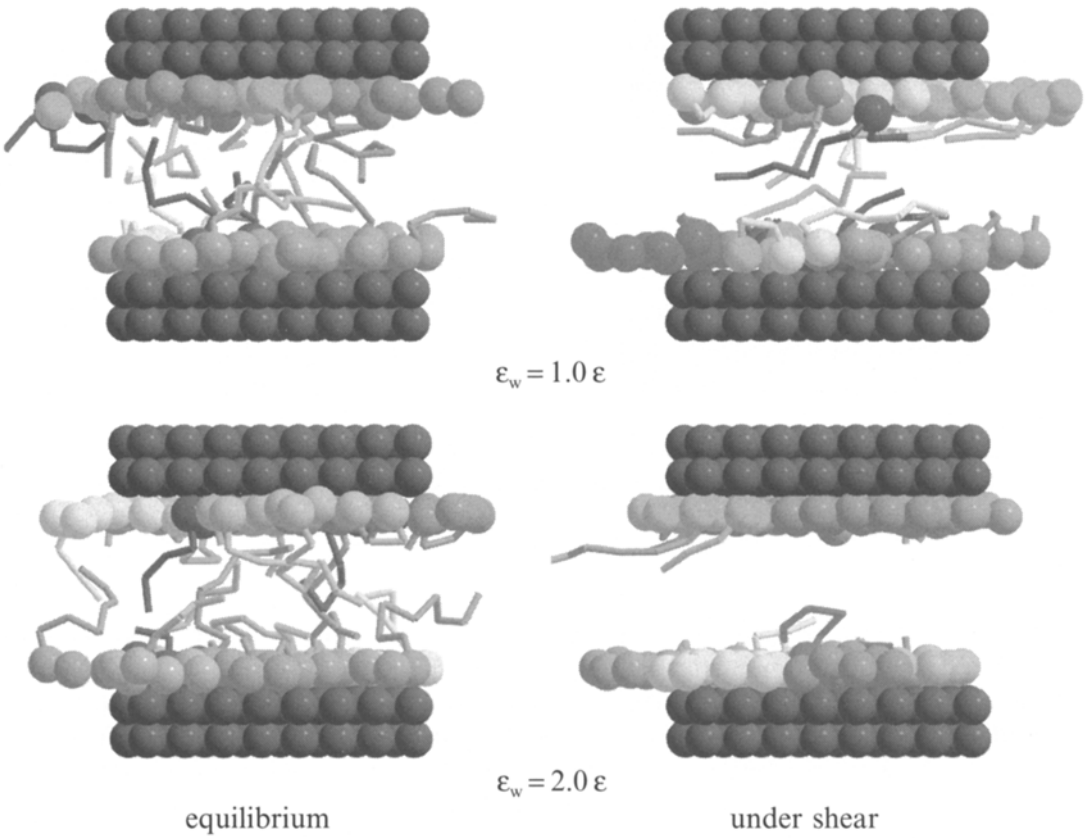

Fig. 4. The adsorbed chain conformations on weakly (top, $\varepsilon_w = 1$) and strongly (bottom, $\varepsilon_w = 2$) physisorbing surfaces for equilibrium and $v_w = 0.9$ (decamers, $h = 6$). The free chains are omitted for clarity. The adsorbed segments are presented by balls ('beads') and the tails belonging to partly adsorbed chains by cylindrical bonds ('springs'). A projection of the system on the **xz** shear plane is shown. It is obvious that for the $\varepsilon_w = 1$ surfaces there is still a substantial number of adsorbed chains, even at this high shear rate, whereas for $\varepsilon_w = 2$ there are almost no partly adsorbed chains to 'tie' the adsorbed and the free part of the film. This is the molecular mechanism of interlayer slippage.

result, slippage appears at the wall. Even simple LJ fluids exhibit wall slip near a neutral or weakly physisorbing surface [28–31]. In these systems the connectivity inside the fluid is due to the interparticle attraction of the LJ potential (intrinsic cohesion). In the case of long polymer melts, the connectivity is provided by the entanglements between adsorbed and free chains [32,36,37]. In our case, there is no attraction in the interchain potential used (Eq. 1) and even our longer oligomers (20-mers) are below the entanglement length (~30 monomers [13]). However, there is a physical connectivity that arises from the existence of partly adsorbed chains, which are partially inside the first layer, in contact with the surfaces (adsorbed part), and partially extending inside the middle part of the film (Table 2 and Fig. 4). The free tails belonging to partly adsorbed chains bind, i.e. physically connect the adsorbed layers to the slower-moving middle part of the film and prevent it from following exactly the motion of the surfaces (the velocity of the first layer is smaller than the wall velocity), thus giving rise to a slip between the wall and the fluid.

On the other hand, near strongly physisorbing surfaces there is no slip at the wall, but inside

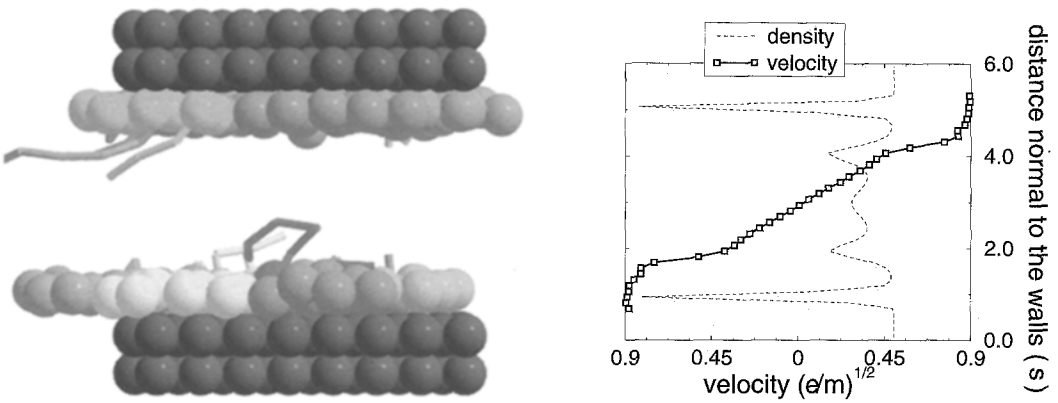

Fig. 5. The adsorbed chain conformations (decamers, $h=6$, $\varepsilon_w=2$) for a high shear rate ($v_w=0.9$). For this $\dot{\gamma}$, nearly all physical connectivity between the first layer and the middle part is lost and slippage takes place inside the fluid. The corresponding velocity profile reveals the locking of the interfacial chains on the confining wall, whereas at the same time an interlayer slip develops between the adsorbed chains and the middle part of the film. The perpetual exchange of chains (adsorption–desorption process) is the only mechanism that prevents a complete slip to take place and induces flow in the central part of the system.

the film there is a change from no slip, at low shear rates, to the development of considerable interlayer slip at higher $\dot{\gamma}$. Inside the film: (i) for small shear rates, still a sufficient number of partly adsorbed chains is present (Table 2), acting as *connectors* between the adsorbed layer and the middle part of the film, thus hindering any interlayer slip [16,17]; and (ii) for the higher shear rates, the adsorbed chains stretch and align parallel to the walls so strongly that nearly all the tails disappear and the physical connectivity provided by them is almost completely lost (Table 2 and Figs. 4 and 5). This results in the appearance of a substantial interlayer slip, with the slip plane located in the region between the adsorbed chains and the middle part of the film, where the free chains are located (Fig. 5). In these systems the adsorbed layer covers the strongly adsorbing surface and locks on it, traveling with the velocity of the wall, so effectively the wall-adsorbed layer system behaves like a neutral wall that moves with respect to the free chains. So, this interlayer slip is completely analogous to the slip near nonadsorbing walls, as the middle part can be considered as a confined oligomer melt between two neutral ($\varepsilon_w=0$) surfaces, where the confining surfaces now are provided by the adsorbed layers that cover the strongly adsorbing solid, screening any attraction from the underlying wall. The difference is that in this case there is some effective roughness of the surface by means of a perpetual chain exchange between adsorbed chains that desorb and free chains that take their place [14,15]. This continuous exchange through the desorption–adsorption process sustains a weak physical connectivity between an effectively neutral surface and a melt of free chains, preventing complete slip from taking place, as it would do next to a neutral smooth solid surface.

In shearing SFA experiments, Horn et al. [24] used an algorithm based on the Chan and Horn method [38] to evaluate the viscous forces in systems of confined PDMS between mica*, and

*There is very strong adhesion between PDMS and mica: in our reduced units the energy of interaction would correspond to values of ε_w higher than 3 [11].

agreement with their SFA results was obtained only 'when stick boundary conditions apply at a distance of 1.5 nm from each surface' and thus 'the shear plane is located inside the film'. Although the above conclusions were derived by fitting equations to experimental data, the physical justification provided for this assumption is extremely close to what is found from the MD simulations reported in the present paper. Horn et al. proposed a 'pinning effect' of the adsorbed chains, resulting in very slow dynamics and 'immobilisation' of the adsorbed chains, and at the same time a physical connection in the form of 'entanglements' between tails and loops of the adsorbed chains and the free chains (Ref. 24, p. 6772ff). Brochard and De Gennes (BG) have recently developed a theory [36,37] describing the response to flow of a melt near a strongly adsorbing surface. From their approach, strong slip is expected near smooth nonadsorbing or weakly adsorbing surfaces, whereas for stronger wall affinities some chains will bind strongly to the surface, creating a 'fluffy carpet' offering a physical link with the chemically identical melt, suppressing any slippage. With increasing shear rates there is a nonslippage to slippage transition through a coil stretch of the adsorbed chains that disentangle from the melt, thus allowing slip to take place.

CONCLUSIONS

Non-equilibrium molecular dynamics simulations have been carried out in order to gain some insight in the nature of flow in nanoscopically confined films. The origin of density inhomogeneities in the vicinity of a confining surface is explained with the help of an 'effective potential', analogous to the one used to demonstrate the radial pair distribution function of a liquid. When flow is introduced to these ultra-confined oligomer melts, slip appears and its position is determined by the confining surface energetics. It is observed that with increasing wall affinity there is a very strong slippage at the wall (neutral walls), which is reduced with increasing ε_w (moderately attractive walls) and disappears completely for stronger interactions ($\varepsilon_w > 2.0$). At the same time, an interlayer slip appears between the adsorbed layer and the middle part of the film, where the free chains are located. A molecular mechanism, involving shear-induced conformational changes of the adsorbed chains, is proposed to account for this slippage taking place inside the fluid films.

REFERENCES

1 Singer, I.L. and Pollock, H.M. (Eds.), Fundamentals of Friction, NATO ASI Series, Vol. 220, Kluwer, Dordrecht, The Netherlands, 1992.
2 Bhushan, B., Tribology and Mechanics of Magnetic Storage Devices, Springer, New York, NY, 1990.
3 Nanotribology, Mater. Res. Soc. Bull., XVIII (1993).
4 Bhushan, B., Israelachvili, J.N. and Landman, U., Nature, 374 (1995) 607.
5 Mate, C.M., McClelland, G.M., Erlandsson, R. and Chiang, S., Phys. Rev. Lett., 59 (1987) 1942.
6 Gee, M.L., McGuiggan, P.M., Israelachvili, J.N. and Homola, A.M., J. Chem. Phys., 93 (1990) 1895.
7 Reiter, G., Demirel, L. and Granick, S., Science, 263 (1994) 1741.
8 Hirz, S.J., Homola, A.M., Hadziioannou, G. and Frank, C.W., Langmuir, 8 (1992) 328.
9 Bitsanis, I. and Hadziioannou, G., J. Chem. Phys., 92 (1990) 3827.
10 a. Thompson, P.A., Grest, G.S. and Robbins, M.O., Phys. Rev. Lett., 68 (1992) 3448.
b. Thompson, P.A., Grest, G.S. and Robbins, M.O., J. Isr. Chem., 35 (1995) 93.
11 Bitsanis, I. and Pan, C., J. Chem. Phys., 99 (1993) 5520.

12 Grest, G.S. and Kremer, K., Phys. Rev., A33 (1986) 3628.
13 Kremer, K. and Grest, G., J. Chem. Phys., 92 (1990) 5057.
14 Manias, E., Hadziioannou, G. and Ten Brinke, G., J. Chem. Phys., 101 (1994) 1721.
15 Manias, E., Subbotin, A., Hadziioannou, G. and Ten Brinke, G., Mol. Phys., 85 (1995) 1017.
16 Manias, E., Hadziioannou, G., Bitsanis, I. and Ten Brinke, G., Europhys. Lett., 24 (1993) 99.
17 a. Manias, E., Hadziioannou, G. and Ten Brinke, G., Langmuir, special issue on tribology, (1996) in press.
b. Manias, E., Bitsanis, I., Hadziioannou, G. and Ten Brinke, G., Europhys. Lett., 33 (1996) 371.
18 Berendsen, H.J.C., Postma, J.P.M., Van Gunsteren, W.F., Di Nola, A. and Haak, J.R., J. Chem. Phys., 81 (1984) 3684.
19 McQuarrie, D.A., Statistical Mechanics, Harper and Row, New York, NY, 1976.
20 Bitsanis, I., Magda, J.J., Tirell, M. and Davis, H.T., J. Chem. Phys., 87 (1987) 1733.
21 Horn, R.G. and Israelachvili, J.N., J. Chem. Phys., 75 (1981) 1400.
22 Christenson, H.K., J. Chem. Phys., 78 (1983) 6906.
23 Horn, R.G. and Israelachvili, J.N., Macromolecules, 21 (1988) 2836.
24 Horn, R.G., Hirz, S.J., Hadziioannou, G., Frank, C.W. and Catala, J.M., J. Chem. Phys., 90 (1989) 6767.
25 a. Davis, H.T., Bitsanis, I., Vanderlick, T. and Tirell, M., American Chemical Society Symposium Series, Vol. 353, American Chemical Society, Washington, DC, 1987, p. 257.
b. Bitsanis, I., Vanderlick, T., Tirell, M. and Davis, H.T., J. Chem. Phys., 89 (1988) 3152.
26 a. Pozhar, L.A. and Gubbins, K.E., J. Chem. Phys., 94 (1991) 1367.
b. Pozhar, L.A. and Gubbins, K.E., J. Chem. Phys., 99 (1993) 8970.
27 Churchill, S.W., Viscous Flows, Butterworth, Boston, MA, 1988.
28 Bitsanis, I., Magda, J.J., Tirell, M. and Davis, H.T., J. Chem. Phys., 87 (1987) 1733.
29 Bitsanis, I., Somers, S., Davis, H.T. and Tirell, M., J. Chem. Phys., 93 (1990) 3427.
30 Somers, S. and Davis, H.T., J. Chem. Phys., 96 (1992) 5389.
31 Heinbuch, U. and Fischer, J., Phys. Rev., A40 (1989) 1144.
32 De Gennes, P.G., Compt. Rend. Acad. Sci., 228B (1979) 219 (also included in Ref. 33).
33 De Gennes, P.G., Simple Views on Condensed Matter, World Scientific, Singapore, 1992.
34 Brochard, F. and De Gennes, P.G., J. Phys. Lett., 45 (1984) L-597.
35 De Gennes, P.G., Introduction to Polymer Dynamics, Cambridge University Press, Cambridge, U.K., 1990.
36 Brochard, F. and De Gennes, P.G., Langmuir, 8 (1992) 3033.
37 Brochard, F., De Gennes, P.G., Hervet, H. and Redon, C., Langmuir, 10 (1994) 1566.
38 Chan, D.Y.C. and Horn, R.G., J. Chem. Phys., 83 (1985) 5311.